UNCLASSIFIED

SECURITY CLASSIFICATION OF THIS PAGE

(4)

REPORT DOCUMENTATION PAGE

AD-A198 800

1b. RESTRICTIVE MARKINGS
NA

3. DISTRIBUTION/AVAILABILITY OF REPORT
Distribution Unlimited; Approved for Public Release

4 PERFORMING ORGANIZATION REPORT NUMBER(S)
INDU/DC/GMH/TR-88-28

5. MONITORING ORGANIZATION REPORT NUMBER(S)
NA

6a. NAME OF PERFORMING ORGANIZATION
Indiana University

6b. OFFICE SYMBOL (If applicable)
NA

7a. NAME OF MONITORING ORGANIZATION
ONR

6c. ADDRESS (City, State, and ZIP Code)
Department of Chemistry
Bloomington, IN 47405

7b. ADDRESS (City, State, and ZIP Code)
800 N. Quincy Street
Arlington, VA 22217

8a. NAME OF FUNDING/SPONSORING ORGANIZATION

8b. OFFICE SYMBOL (If applicable)

9 PROCUREMENT INSTRUMENT IDENTIFICATION NUMBER
Contract N00014-86-K-0366

8c. ADDRESS (City, State, and ZIP Code)

10. SOURCE OF FUNDING NUMBERS

PROGRAM ELEMENT NO.	PROJECT NO.	TASK NO.	WORK UNIT ACCESSION NO
		R&T Code 4134006	

11 TITLE (Include Security Classification)
Detection of Ions by Replacement-Ion Chromatography Coupled to a Microwave-Induced Nitrogen Discharge at Atmospheric Pressure

12 PERSONAL AUTHOR(S)
Leonard J. Galante, Daniel A. Wilson, and Gary M. Hieftje

13a TYPE OF REPORT	13b. TIME COVERED	14. DATE OF REPORT (Year, Month, Day)	15 PAGE COUNT
Technical	FROM ____ TO ____	July 11, 1988	27

16. SUPPLEMENTARY NOTATION
Accepted for publication in Analytica Chimica Acta

17 COSATI CODES		
FIELD	GROUP	SUB-GROUP

18 SUBJECT TERMS (Continue on reverse if necessary and identify by block number)
Ion Chromatography, Spectroscopic Detection, Speciation, Multielement Analysis, Microwave Plasma,

19. ABSTRACT (Continue on reverse if necessary and identify by block number)

The capabilities and limitations of replacement-ion chromatography (RIC) employing a lithium-based replacement method and a microwave-induced nitrogen discharge at atmospheric pressure (MINDAP) as the detector are critically evaluated for the determination of anions and cations. The system, including chromatographic columns, interface, and plasma-emission source provides absolute detection limits of 30-300 ng for anions and 100-500 ng for cations. Detectability and precision of the instrument are ultimately limited by multiplicative noise sources. The limitations imposed by multiplicative noise on RIC detection are assessed, and guidelines are presented that will allow judicious choice of alternative RIC detectors in the future.

20. DISTRIBUTION/AVAILABILITY OF ABSTRACT
☒ UNCLASSIFIED/UNLIMITED ☐ SAME AS RPT ☐ DTIC USERS

21 ABSTRACT SECURITY CLASSIFICATION
Distribution Unlimited

22a NAME OF RESPONSIBLE INDIVIDUAL
Gary M. Hieftje

22b TELEPHONE (Include Area Code)
(812) 335-2189

22c OFFICE SYMBOL

DD FORM 1473, 84 MAR 83 APR edition may be used until exhausted
All other editions are obsolete

SECURITY CLASSIFICATION OF THIS PAGE

UNCLASSIFIED

OFFICE OF NAVAL RESEARCH

Contract N14-86-K-0366

R&T Code 4134006

TECHNICAL REPORT NO. 28

DETECTION OF IONS BY REPLACEMENT-ION CHROMATOGRAPHY COUPLED TO A MICROWAVE-INDUCED NITROGEN DISCHARGE AT ATMOSPHERIC PRESSURE

by

Leonard J. Galante, Daniel A. Wilson, and Gary M. Hieftje

Accepted for Publication

in

ANALYTICA CHIMICA ACTA

Indiana University
Department of Chemistry
Bloomington, Indiana 47405

11 July 1988

INTRODUCTION

In previous work, our research group introduced [1] and characterized [2] a new detection method for high-performance ion chromatography (HPIC) called replacement-ion chromatography (RIC). The method employs equipment and columns similar to those in suppressed-ion chromatography [3-5] but uses also a third column to replace eluting solute ions (or their co-ions) with another ionic species (the replacement ion). The replacement ion is then monitored by an appropriate detector.

Importantly, RIC offers versatility because it can employ vertually any detector that is compatible with a liquid chromatograph and sensitive to a suitable replacement ion. Our previous investigations have explored flame-spectrometric [1,2] and UV-spectrophotometric [6] detection. However, it has been difficult to attain low detection limits with certain eluents by flame-emission detection because these eluents produce a high background replacement ion concentration in the column effluent [1,2].

In an effort to improve detection limits, another sensitive spectroscopic source, the microwave-induced nitrogen discharge at atmospheric pressure (MINDAP) [7-9], was coupled to a Li^+-based RIC system. This source provided RIC detection limits of 30-300 ng for several common anions and 100-500 ng for alkali-metal cations. Although these values are not superior to those observed with a simple flame source [2] and are far poorer than the MINDAP can deliver by itself [7-9], our results are reported here to illustrate and explain the importance of multiplicative noise in an RIC system. In addition, guidelines are provided that will help future investigators choose

detectors for RIC based on fundamental principles rather than empirical testing. Calibration equations for several ions are also presented.

EXPERIMENTAL

A schematic diagram of the detection system used in this study appears in Figure 1.

Chromatographic Equipment

The liquid chromatograph included a minipump® (model 396, Milton Roy Co., Riviera Beach, FL) equipped with pulse dampener and injection valve (model 7010, Rheodyne, Cotati, CA). The injection valve was equipped with a 20-μl sample loop. The commercial columns used in this study were all Dionex products. Columns used for anion separations included an anion guard column (model 30986), separator column (model 30985), and suppressor column (model 30828). Columns used for cation separations included a cation guard column (model 35370), separator column (model 35371), and suppressor column (model 30834). The lithium replacement column consisted of a Nafion® cation-exchange fiber housed in a reservoir, which accommodated the continuously flowing salt solution (regenerant) used to maintain the fiber in the desired ionic form. The fiber is approximately 1.5 m in length, packed with inert glass beads, and sold commercially by Dionex (model 35350) for use as a fiber-eluent suppressor (Dionex Product Document, No. 800-032157). This column can be adapted easily for use as a cation-replacement column [2]. All columns were connected by 1.6-mm o.d. x 0.3-mm i.d. Teflon tubing with Omnifit (Atlantic Beach, NY) polypropylene tube-end bushings and grippers.

Replacement Column-Plasma Interface

A 60-mm long x 1.6-mm o.d. x 0.3-mm i.d. Teflon tube was connected to the outlet of the replacement column with an Omnifit bushing and gripper. The open end of the Teflon tube was inserted into the glass sample tube (inner tube) of a concentric glass nebulizer (laboratory built) until the end of the plastic tube fit snugly into the tapered conical tip of the sample tube. The replacement-column outlet and the nebulizer were held firmly in place with clamps. The approximate void volume between the end of the plastic tube and the tip (outlet) of the nebulizer was 75 μl.

Column effluent was nebulized into the plasma through a conventional pneumatic nebulizer-spray chamber arrangement; the nebulizer was operated at a nitrogen flow rate of 2.3 L/min, and the aerosol was then passed through a double-pass spray chamber (laboratory constructed).

The plasma will accept and decompose wet aerosols, but background and noise levels are lower when aerosols are desolvated [8]. Consequently, the aerosol leaving the spray chamber was directed through a desolvation system that included a heated glass tube to dry the aerosol and a condenser to remove most of the water vapor [10]. The glass tube (approximately 20-mm o.d. x 150-mm long) was wrapped with 0.5-in. (13-mm) heating tape to maintain the tube at approximately 140 °C. The voltage supplied to the heating tape was controlled by an autotransformer. The condenser (model 9270, Ace Glass Inc., Vineland, NJ) was maintained at approximately 5 °C by a refrigerated recirculating water bath (Multi-cool®, FTS Systems, Inc., Stone Ridge, NY).

The volume of the desolvation system, including heated glass tube and condenser, did not appear to distort the chromatographic peak shape. Generally, peak broadening and peak shape are less affected by transfer volumes following the nebulizer (after the effluent is converted to an aerosol) than by transfer volumes preceding the nebulizer [11].

Microwave-Plasma Emission Spectrometer

The plasma was sustained in a 4-mm i.d. torch (laboratory built) consisting of two concentric quartz tubes and held within a modified TM_{010} cavity. Microwave power was supplied through a double-stub tuner (model DS109, Weinschel Eng., Gaithersburg, MD). These components and other details concerning ignition and tuning of the plasma have been described previously [8]. The 2.3 L/min of nitrogen exiting the condenser and containing dry analyte aerosol was introduced into the tangential inlet (outer tube) of the torch. The nitrogen flow rate through the axial inlet (central tube) of the torch was 0.4 L/min. In the present study, the plasma was operated at an applied power of 210 W at 2450 MHz (Model 420, variable 500 W power supply, Micro-Now Instrument Co., Chicago, IL). The reflected power was approximately 18 W during all experiments.

The plasma was viewed radially (side-on configuration); a 2:1 magnified image of the plasma tail flame was focused with a spherical mirror (MgF_2 overcoat, 108-mm focal length and 108-mm diameter, Oriel Corp., Stamford, CT) onto the entrance slit (50 μm) of a monochromator (model EU-700, 0.35-m f.l., Heath Co., Benton Harbor, MI). The viewing height was approximately 5 mm above the cavity. The monochromator was set at the lithium (I) 670.78 nm emission line. A digital photometer

RESULTS AND DISCUSSION

Anion Determinations

Equimolar solution mixtures of F^-, Cl^-, and Br^- between 1.0 and 25.0 mM were injected and separated with the standard eluent. Each solution was injected three or four times (nonconsecutively). The anions, which elute from the suppressor column associated with an H^+ cation, are converted to their lithium salts in the replacement column and subsequently detected by the plasma. A representative chromatogram illustrating the detection of a 5.0-mM, three-component sample appears in Figure 2.

Reproducibility. At levels well above the detection limit, precision was generally independent of the injected concentration and appeared to be limited by short- and long-term drift of the plasma source. Much of this instability appeared to be caused by drift in the applied and reflected microwave power. Peak-height relative standard deviations (RSDs) for F^-, Cl^-, and Br^- were typically 5.0 - 8.0% (3-4 injections). Peak-area RSDs were typically 8.0 - 13%, appreciably larger than those observed previously in RIC with a flame-emission detector [2].

Sensitivity. Peak-height and peak-area calibration curves were generated to assess linearity and relative sensitivity (slope) over the explored concentration range (1.0 - 25 mM). These results are summarized in Table 1.

Conceptually, all ions should produce an equivalent integrated RIC response because only the replacement ion, Li^+, is detected. However, the slopes reported in Table 1 for F^- and Br^- are lower than that of Cl^-

(model 124, Pacific Precision Instruments, Concord, CA) was used to maintain a -800 V bias across the PMT (R928, Hamamatsu Co., Middlesex, NJ) and to convert the PMT photocurrent to a proportional voltage. The time constant of the photometer was set at 1.0 second. Chromatograms were recorded on a strip-chart recorder (model SR-204, Heath Co., Benton Harbor, MI) and by MINC-11/23 computer (Digital Equipment Corp., Maynard, MA). Peaks were later integrated with the MINC computer.

Reagents

Salts or acids used to prepare eluents, regenerant solutions, and ion samples were either analytical or A.C.S. reagent grade (Mallinchrodt, St. Louis, MO or MCB, Cincinnati, OH). The water used in all experiments was distilled and deionized.

Procedures

The outside of the fiber (replacement column) was continuously bathed with a regenerant solution containing 0.025 N Li^+ as Li_2SO_4. The regenerant flow rate was maintained at 2.5 ml/min countercurrent to column flow and regulated by gravity. Other experimental details concerning the preparation of suppressor columns and the performance characteristics of the replacement column are reported elsewhere [2].

All separations were performed at an eluent flow rate of 2.0 ml/min. Anions were separated using the standard eluent [4], 2.4 mM Na_2CO_3 and 3.0 mM $NaHCO_3$. Cations were separated with 0.005 N HNO_3. Synthetic ion samples were prepared in mobile phase and contained equimolar concentrations of either F^-, Cl^-, and Br^-, or Li^+, Na^+, and K^+. The injected sample volume was 20 μl.

The detection limits of F^-, Cl^-, and Br^- were defined as the injected concentration that would provide a signal-to-noise ratio (S/N) of 2. Here signal refers to the net signal of each eluting component (peak) in the chromatogram and noise refers to the root-mean-square value of the baseline fluctuation (approximately equivalent to one fifth the peak-to-peak fluctuation of the baseline).

by 20% and 14%, respectively. At high concentrations, the peak areas of Br^- are consistently lower than those of Cl^- by an average of 18%, which suggests a systematic loss of Br^-. Previous studies [2] indicate that the highly retained bromide ion is partially adsorbed by the separator column.

In contrast, the disparity between F^- and Cl^- peak areas increases gradually with concentration. This trend is shown in Table 2, which lists the mean peak areas of the two anions and their ratio at each injected concentration. The lower response to F^- relative to Cl^- has been attributed to the partially nonionic character of the fluoride conjugate acid, HF [2]. Anions that form weak acids in the suppressor column are not completely excluded from the suppressor-column resin or the fiber ionomer. Accordingly, weak acids experience additional band broadening in these columns and can produce a low, nonstoichiometric response via several possible mechanisms [2].

Detection Limits. Detection limits ($\mu g\ ml^{-1}$ and ng) for F^-, Cl^-, and Br^- are presented in Table 3. When presented in units of absolute mass, these detection limits are about a factor of 1.5 greater (worse) than those obtained with the flame-emission source under similar chromatographic conditions. This difference is probably not significant, based on the inherent uncertainty in detection limits.

Cation Determinations

Equimolar solution mixtures of Li^+, Na^+, and K^+ between 0.5 mM and 25.0 mM were injected sequentially from low to high concentration; the sequence was then repeated. The cations, which elute from the suppressor column as their hydroxide salts, are all converted to lithium hydroxide

in the replacement column and subsequently detected with the plasma. A representative chromatogram illustrating the detection of a 5.0 mM multielement sample appears in Figure 3.

Although good signal to baseline noise is observed at higher concentrations of cations (cf. Figure 3), peak height decreases disproportionately with concentration below 2.5 mM. In fact, RIC signals disappear into the baseline at injected concentrations of 1.0 mM or less. Peaks are also unusually asymmetric and exhibit considerable tailing. Similar results were observed with the flame-emission detector and have been attributed to physicochemical interactions between the cation hydroxide solutes and the cation-exchange material of the replacement column [2].

Reproducibility. Peak areas and peak heights were unusually irreproducible for cations, particularly at concentrations barely above 1.0 mM. Occasionally, peak heights decreased or increased by more than 50% between replicate injections. Precision improved as the injected concentration increased. For example, the relative mean deviations of peak heights varied from 23 to 57% at injected concentrations between 2.5 mM and 4.0 mM, from 12 to 24% at concentrations between 4.0 mM and 15.0 mM, and from 1 to 8% at concentrations between 15.0 mM and 25.0 mM.

Sensitivity. Peak-height calibration curves for Li^+, Na^+, and K^+ exhibited negative curvature above sample concentrations of 10.0-15.0 mM whereas peak-area working curves were reasonably linear over the entire observed concentration range (2.5-25 mM). The peak-area and peak-height calibration equations appear in Table 4.

Interestingly, the intercepts of all working curves in Table 4 are large and negative and appear to reflect the signal loss that was

observed at sample concentrations below 1.0 mM. In fact, all the equations intersect the concentration axis at approximately 1.0 mM. The slopes of the peak-area working curves (Table 4) are similar and indicate that the integrated detector response is nearly equivalent (universal) for the three cations.

Detection Limits. Detection limits for ($\mu g\ ml^{-1}$ and ng) for Li^+, Na^+, and K^+ are reported in Table 3. Each value in Table 3 was determined from the respective peak-height calibration equation (Table 4) and corresponds to the concentration at a peak-height of zero. This unusually defined limit of detection is approximately 1.0 mM and is caused by the chemical interaction discussed above.

Importance of Multiplicative Noise

Most of the observations described above can be understood by recognizing the importance of multiplicative detector noise in an RIC system. To demonstrate the significance of multiplicative noise, the detection limit of lithium was evaluated in the presence of only plasma background (without the lithium background encountered in RIC). A flow-injection procedure was employed in which six 20-μl aliquots of a 10 ppb Li^+ (1.4×10^{-6} M) solution were injected into a prepared column (containing an anion-exchange resin) and eluted with distilled water (2.0 ml/min). Lithium injected in this manner is not retained but rapidly passes through the system. The average signal-to-baseline noise ratio (S/N) for these injections was 12; the extrapolated detection limit (S/N = 2) is therefore 1.7 ppb or 2.4×10^{-7} M, three orders of magnitude better than the values reported in Table 3. Of course, this disparity is caused in part by the increased chromatographic dilution

experienced by the separated components in RIC. However, the unusually large RIC detection limits are caused principally by instability in the large background Li^+ signal produced by the standard eluent [2].

This signal instability can be more clearly understood by considering the dominant noise sources inherent in the plasma-based-detection system. At high analyte concentrations, the fluctuation (noise) in the signal is dominated by analyte flicker at frequencies below 1 Hz [12]. This flicker noise can arise from a variety of sources in the system, including plasma waver, nebulizer variation, and generator instability and has been characterized earlier [12]. The microwave power supply appears to be a significant noise source, and fluctuations in emission signals have been correlated with those in the applied power [12]. For example, at an applied power setting of 210 W, the applied-power meter of the generator fluctuates $\pm$ 3 W. This power instability contributes, in part, to the fluctuation of the background lithium signal in RIC.

Unfortunately, this fluctuation is a form of multiplicative noise and therefore difficult to remove; it is 1/f in character and is proportional to the signal amplitude [12, 13]. As a result, the varying amplitude of the background Li^+ signal in RIC cannot be reduced by increasing the time constant of the detection system. In fact, in the plasma source, noise is minimal at time constants between one and five seconds [12]. Moreover, because analyte-flicker noise increases in proportion to the signal, RIC detection limits are strongly dependent upon the background Li^+ concentration. In a flicker-noise-limited emission measurement, equation 1 applies [14].

$$S/N \propto i_s/k\bar{i}_b \qquad (1)$$

Here, i_s = signal current, $\bar{i}_b$ = average background current, and k = the flicker factor (a measure of the amount of multiplicative noise inherent in the background signal). In the RIC experiment, $\bar{i}_b$ is the photocurrent produced by background Li^+ and i_s is the net signal produced by an eluting peak ($i_{peak} - \bar{i}_b = i_s$). Equation 1 predicts an inverse relationship between S/N and background level and explains why the anion detection limits in Table 3 are much higher than the lithium detection limit obtained in the presence of only plasma-background emission (~ 2ppb).

The background signal (from background lithium ions) produced by the nitric acid eluent (cation eluent) is about an order of magnitude lower than that produced by the standard carbonate eluent (anion eluent) [2]. Consequently, the baseline-noise amplitude in cation chromatograms is proportionally lower (cf. Figures 2 and 3). This behavior confirms our conclusion that detection limits in these RIC experiments are limited by multiplicative analyte-flicker noise in the plasma source. Unfortunately, the detection limits for cations do not improve by an order of magnitude as predicted by equation 1, because of the previously discussed chemical interactions that occur in cation determinations.

Other RIC Detectors

Unfortunately, the detection limits obtained for anions with the MINDAP (Table 3) or with flame detectors [1, 2] are about an order of magnitude larger

than those reported for the conductivity detector [4, 5]. Although superior detection limits have not been obtained with our Li^+-based arrangement, an alternative scheme employing a different replacement cation or detector might provide better results. The creation of an alternative and successful RIC detection system requires the choice and effective integration of three fundamental components: the replacement column, replacement ion, and detector. The important considerations below will help guide future investigators in the design of alternative RIC systems.

Replacement Column. Ideally, the replacement column should operate continuously, efficiently, reproducibly, and introduce minimal dead volume. We have shown that fiber-based-replacement columns adequately fulfill these requirements [2, 6].

Replacement Ion. The replacement ion should have a low affinity for the charged sites of the replacement column compared to that of the solute ion which is replaced [2, 6]. A monovalent replacement ion is most desirable to maximize detector signal.

Detector. The detector must respond selectively and sensitively to the replacement ion, so universal calibration and low detection limits are realized. As the present study demonstrates, a sensitive detector will not guarantee low RIC detection limits if a large background-replacement-ion concentration exists and if the detector is plagued by multiplicative noise. Accordingly, it is optimal not to identify the most sensitive detector but rather the one that has good sensitivity and the lowest flicker factor (equation 1). Unfortunately, it is difficult to predict the sensitivity of some detection systems under RIC conditions without empirical testing, because flicker factors might not

be defined for a given instrument or set of operating conditions. Moreover, the detection limits of most systems will often depend upon how well the detection system can be stabilized. For example, both short-term (high frequency) and long-term (drift) fluctuation of the plasma signal might be reduced by further stabilization or filtering of the microwave power supply.

For some detectors, RIC detection limits can be estimated from precision measurements obtained at analyte concentrations that are similar in magnitude to typical RIC background levels. One first applies equation 2 [15],

$$\frac{S}{N} = \frac{1}{RSD} \qquad (2)$$

where N refers to the noise amplitude on the analyte signal, S. Thus, if the precision of a detector is 1% at an analyte concentration of 0.4 mM (a typical background replacement-ion concentration encountered with the standard anion eluent), the standard deviation of the signal is equivalent to an analyte concentration of 0.004 mM. The detection limit can then be defined as three times the standard deviation of the background signal, which in this case is 0.012 mM. Therefore, a peak concentration of 12 μM could be distinguished from fluctuations in the baseline and represents a reasonable estimate of the detection limit with this hypothetical RIC system.

It is important to recognize that detection limits based on precision measurements are likely to be somewhat overestimated because the precision of an analytical system is often measured over a relatively long period of time. Consequently, these measurements often

reflect the signal fluctuation caused by system drift as well as that caused by short-term noise.

Precision measurements can be used also to evaluate the noise characteristics of a potential RIC detector. If the detection system is dominated by multiplicative noise, both the signal and the noise on the signal increase proportionately with concentration [12]. Consequently, the signal-to-noise (noise on the signal) ratio and therefore precision (RSD) will be independent of analyte concentration (equation 2).

It is even easier to predict RIC detection limits for detectors that have well defined noise characteristics. For example, the user manuals of many commercial spectrophotometric instruments and other reference sources [16] provide noise levels in absorbance units at selected wavelengths and specified background levels for HPLC UV-VIS absorption detectors. In addition, the absolute signal (absorbance) of such a detector can be easily related to the concentration of an absorber by using Beer's law. This information can be used to predict RIC detection limits for a particular absorber (replacement ion) at known RIC background levels [6].

ACKNOWLEDGEMENTS

The authors thank Dionex Corporation for providing the chromatographic columns used in this study. This research was supported by grants from the National Science Foundation, the Office of Naval Research, and American Cyanamid.

REFERENCES

1 S. W. Downey and G. M. Hieftje, Anal. Chim. Acta, 153 (1983) 1-13.

2 L. J. Galante and G. M. Hieftje, Anal. Chem., 59 (1987) 2293-2302.

3 C. A. Pohl and E. L. Johnson, J. Chromatogr. Sci., 18 (1980) 442-452.

4 J. S. Fritz, D. T. Gjerde and C. Pohlandt, Ion Chromatography, Dr. Alfred Hüthig Verlag, Heidelberg, West Germany, 1982.

5 F. C. Smith, Jr., R. C. Chang, The Practice of Ion Chromatography, John Wiley & Sons, New York, 1983.

6 L. J. Galante and G. M. Hieftje, Anal. Chem., submitted for publication, 1987.

7 A. T. Zander and G. M. Hieftje, Appl. Spectrosc., 35 (1981) 357-371.

8 R. D. Deutsch and G. M. Hieftje, Appl. Spectrosc., 39 (1985) 214-222.

9 R. D. Deutsch, J. P. Keilsohn and G. M. Hieftje, Appl. Spectrosc., 39 (1985) 531-534.

10 C. Veillon and M. Margoshes, Spectrochim. Acta, 23B (1968) 553-555.

11 B. S. Whaley, K. R. Snable and R. F. Browner, Anal. Chem., 54 (1982) 162-165.

12 R. D. Deutsch and G. M. Hieftje, Appl. Spectrosc., 39 (1985) 19-24.

13 M. S. Epstein and J. D. Winefordner, Prog. Anal. At. Spectrosc., 7 (1984) 67-137.

14 C.Th.J. Alkemade, W. Snelleman, G. D. Boutilier, B. D. Pollard, J. D. Winefordner, T. L. Chester and N. Omenetto, Spectrochim. Acta, 33B (1978) 383-399.

15 G. M. Hieftje, Anal. Chem., 44 (1972) 81A-88A.

16 R. L. Stevenson, in T. M. Vickrey (Ed.), Liquid Chromatography Detectors, Chromatographic Science Series, Vol. 23, Marcel Dekker, New York, 1983, pp. 80-83.

Table 1: Linear Least-Squares Parameters for fits of Peak-Area and Peak-Height Response (arbitrary units) Versus Concentration (M) for Several Anions.

Anion	Least-Squares Slope	Least-Squares Intercept	Correlation Coefficient	Standard Error of Estimate
Peak-Area Working Curve				
F^-	2355 ± 42	0.06 ± 0.46	0.999	0.85
Cl^-	2948 ± 57	-1.53 ± 0.62	0.999	1.15
Br^-	2534 ± 101	-1.55 ± 1.10	0.996	2.02
Peak-Height Working Curve				
F^-	51.9 ± 0.7	0.037 ± 0.008	0.999	0.014
Cl^-	77.0 ± 4.0	0.012 ± 0.023	0.995	0.031
Br^-	20.8 ± 0.6	0.010 ± 0.006	0.998	0.011

Table 2: Mean peak areas (arbitrary units) of Cl^- and F^- and their ratio at each injection concentration.

Concentration (mM)	Cl^- peak area	F^- peak area	F^- to Cl^- peak-area ratio
1.0	2.63	2.68	1.02
2.0	4.63	4.74	1.02
4.0	9.75	9.41	0.97
5.0	13.7	12.6	0.92
7.5	20.3	18.0	0.89
10.0	26.0	22.0	0.85
25.0	73.0	59.3	0.81

Table 3: Detection Limits with RIC Coupled to Atomic-Emission Sources

	Detection Limits			
	RIC-MINDAP		RIC-Flame[a]	
Anions	$\mu g\ ml^{-1}$[b]	ng	$\mu g\ ml^{-1}$[c]	ng
F^-	1.8	36	0.26	26
Cl^-	3.1	62	0.43	43
Br^-	18	370	--	--
Cations	$\mu g\ ml^{-1}$[b]	ng		
Li^+	5.9	120		
Na^+	17	340		
K^+	25	500		

[a]Values obtained from reference 2.

[b]Values obtained with a sample volume of 20 μl.

[c]Values obtained with a sample volume of 100 μl.

Table 4: Linear Least-Squares Parameters for fits of Peak-Area and Peak-Height Response (arbitrary units) Versus Concentration (M) for Several Cations.

Cation	Least-Squares Slope	Least-Squares Intercept	Correlation Coefficient	Standard Error of Estimate
Peak Area				
Li^+	3818 ± 105	-5.11 ± 1.29	0.998	2.04
Na^+	3837 ± 94	-3.47 ± 1.15	0.999	1.81
K^+	3519 ± 57	-3.33 ± 0.70	0.999	1.10
Peak Height				
Li^+	78.1 ± 1.8	-0.065 ± 0.012	0.999	0.011
Na^+	64.7 ± 1.9	-0.048 ± 0.012	0.999	0.011
K^+	18.3 ± 0.4	-0.012 ± 0.003	0.999	0.002

FIGURE CAPTIONS

Figure 1. Schematic diagram of the RIC detection system, including separator, suppressor, and replacement columns and microwave-induced nitrogen discharge.

Figure 2. Chromatogram demonstrating the separation and detection of 5.0 mM F^-, Cl^-, and Br^-. Eluent, 2.4 mM Na_2CO_3 and 3.0 mM $NaHCO_3$ at 2.0 ml/min. Injection volume, 20 μl.

Figure 3. Chromatogram demonstrating the separation and detection of 5.0 mM Li^+, Na^+, and K^+. Eluent, 0.005 N HNO_3 at 2.0 ml/min. Injection volume, 20 μl.

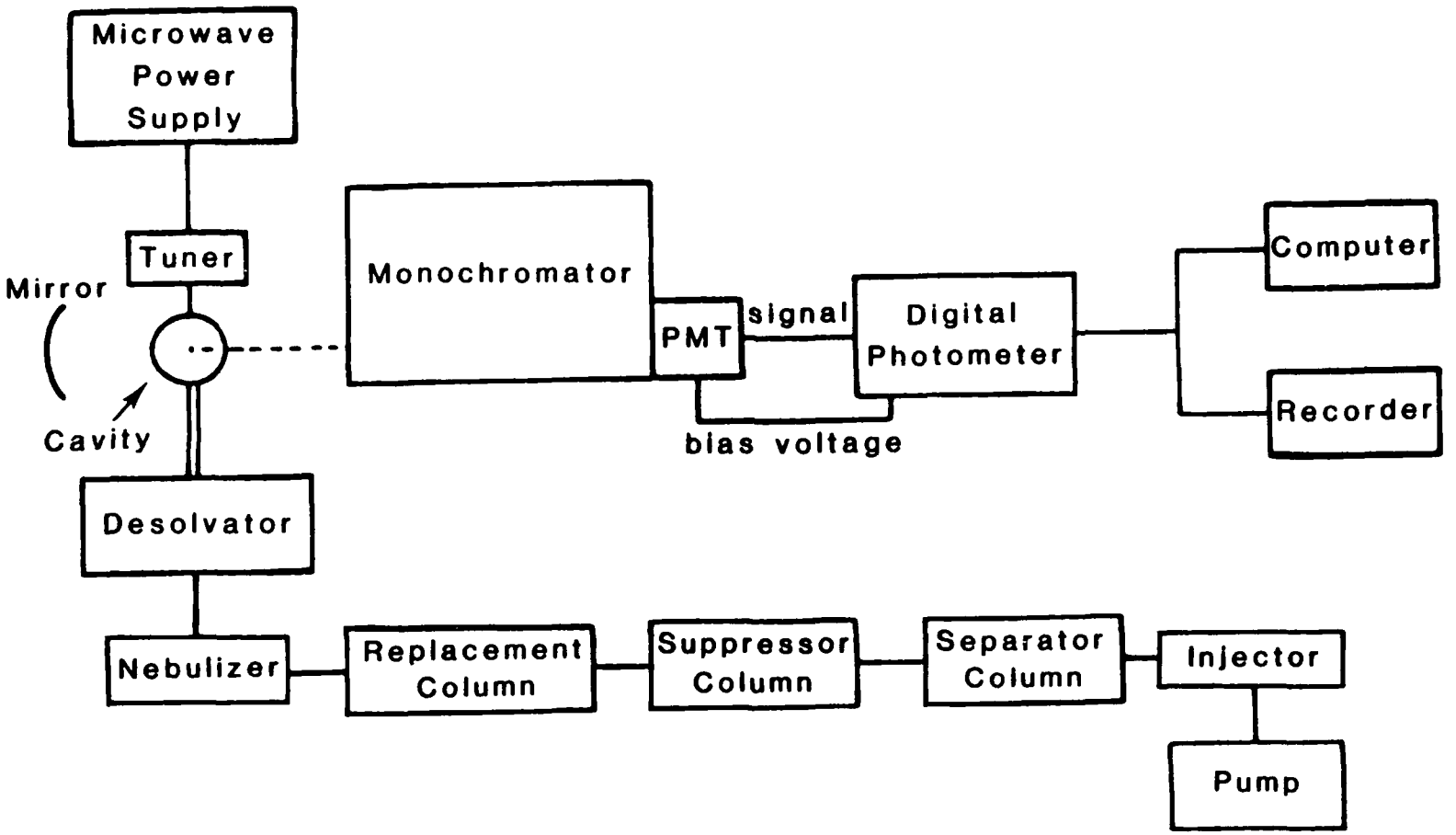
Microwave Power Supply
Tuner
Mirror
Cavity
Monochromator
PMT
signal
Digital Photometer
Computer
Recorder
bias voltage
Desolvator
Nebulizer
Replacement Column
Suppressor Column
Separator Column
Injector
Pump

Fig. 1

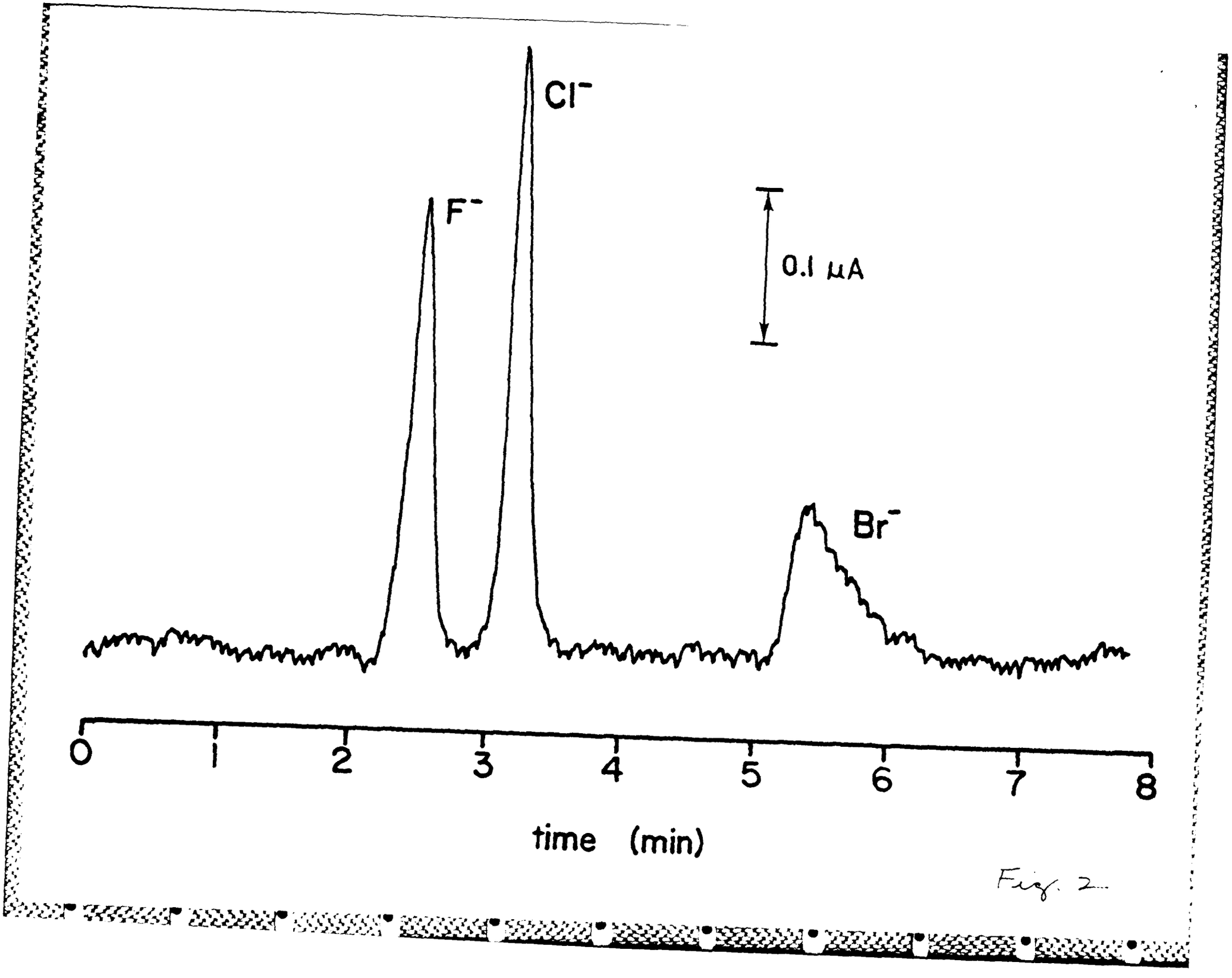

Fig. 2

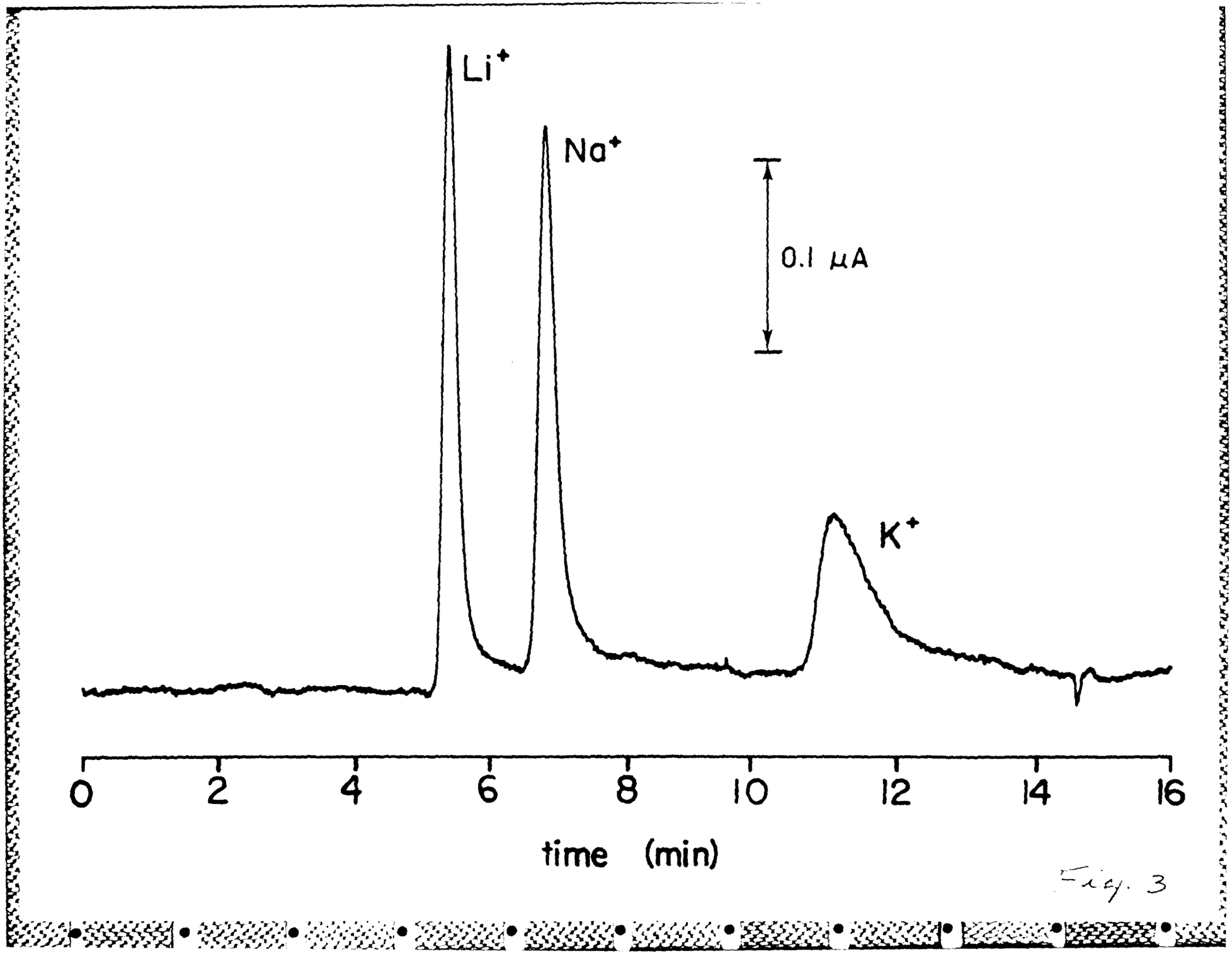

Fig. 3

TECHNICAL REPORT DISTRIBUTION LIST, GEN

	No. Copies
Office of Naval Research Attn: Code 1113 800 N. Quincy Street Arlington, Virginia 22217-5000	2
Dr. Bernard Douda Naval Weapons Support Center Code 50C Crane, Indiana 47522-5050	1
Naval Civil Engineering Laboratory Attn: Dr. R. W. Drisko, Code L52 Port Hueneme, California 93401	1
Defense Technical Information Center Building 5, Cameron Station Alexandria, Virginia 22314	12 high quality
DTNSRDC Attn: Dr. H. Singerman Applied Chemistry Division Annapolis, Maryland 21401	1
Dr. William Tolles Superintendent Chemistry Division, Code 6100 Naval Research Laboratory Washington, D.C. 20375-5000	1
Dr. David Young Code 334 NORDA NSTL, Mississippi 39529	1
Naval Weapons Center Attn: Dr. Ron Atkins Chemistry Division China Lake, California 93555	1
Scientific Advisor Commandant of the Marine Corps Code RD-1 Washington, D.C. 20380	1
U.S. Army Research Office Attn: CRD-AA-IP P.O. Box 12211 Research Triangle Park, NC 27709	1
Mr. John Boyle Materials Branch Naval Ship Engineering Center Philadelphia, Pennsylvania 19112	1
Naval Ocean Systems Center Attn: Dr. S. Yamamoto Marine Sciences Division San Diego, California 91232	1

END

DATE

FILMED

DTIC

11-88